Veterinary Microbiology 307 (2025) 110613

Contents lists available at ScienceDirect

Veterinary Microbiology

journal homepage: www.elsevier.com/locate/vetmic

EEF1D signaling contributes to Bovine alpha herpesvirus 1 productive infection, potentially through regulation of viral replication compartments

Bin Hou, Xiaotian Fu, Yuanshan Luo, Xiuyan Ding *, Liqian Zhu *

Key Laboratory of Microbial Diversity Research and Application of Hebei Province, College of Life Sciences, Hebei University, Baoding 071002, China

ARTICLE INFO

Keywords:
EEF1D
BoAHV1
ICP8

ABSTRACT

Bovine alpha herpesvirus 1 (BoAHV1) is one of the most significant viruses affecting cattle, causing substantial economic losses to the cattle industry worldwide. Eukaryotic translation elongation factor 1δ (EEF1D), a component of the elongation factor 1 complex, plays a crucial role in the elongation phase of protein synthesis. However, the interplay between viral infection and EEF1D signaling remains poorly understood within the virus community. Here, we report that BoAHV1 productive infection leads to increased steady-state protein expression of EEF1D in cell cultures. Immunofluorescence assays demonstrated that productive viral infection in MDBK cells induces the enhanced translocation of EEF1D into the nucleus, where it forms specific puncta and co-localizes with the puncta of viral protein ICP8, a marker of the viral replication compartment. Additionally, viral infection in MDBK cells re-localizes a portion of EEF1D in the cytoplasm, where it co-localizes with the virion-associated proteins, such as viral protein gD. While, co-localization of EEF1D with virion-associated proteins is primarily observed in the nuclei of virus-infected Neuro-2A cells. Moreover, siRNA-mediated knockdown of EEF1D expression significantly decreases BoAHV1 productive infection in MDBK cells. Thus, the association of EEF1D with multiple viral proteins, particularly ICP8, a component of the viral replication compartment, may represent a potential mechanism by which EEF1D regulates viral replication.

1. Introduction

Bovine alpha herpesvirus 1 (BoAHV1), an enveloped DNA virus belonging to the genus *Varicellovirus* in the subfamily *Alphaherpesvirinae* under the family *Herpesviridae* (Muylkens et al., 2007; Tikoo et al., 1995), is one of the most significant viral pathogens affecting cattle farms globally(Petrini et al., 2019; Siddell et al., 2023; Tikoo et al., 1995). Infection with this virus can lead to mucosal lesions in the upper respiratory tract and dampen the host's immune responses (Fulton et al., 2016; Hodgson et al., 2005; Jones and Chowdhury, 2007), thereby facilitating secondary infections by other pathogens. This can result in a severe disease known as the bovine respiratory disease complex (BRDC) (Jones, 2019). Furthermore, BoAHV1 is the most commonly identified pathogen in viral abortions within the North American cattle industry (Chase et al., 2017; Jones, 2019), accounting for 25–60 % of the abortions that occur in cows (Jones, 2019). BoAHV1 infections impose substantial economic losses on the global cattle industry(Iscaro et al., 2021; Muylkens et al., 2007).

The eukaryotic translation elongation factor-1 (EEF1) protein complexes are crucial for protein synthesis, recruiting aminoacylated transfer (t)RNA molecules to ribosomes in a GTP-dependent manner (Dever and Green, 2012). The EEF1 complex is composed of two subunits, EEF1A and EEF1B. EEF1δ (EEF1D), a component of the EEF1B complex, is known to catalyze the exchange of GDP for GTP bound to EEF1A during translation elongation steps (Xie et al., 2020), thereby facilitating protein synthesis by aiding eEF1A1 in recruiting aminoacyl-tRNAs to the 80S ribosome (Andersen et al., 2000; Dever and Green, 2012; Gao et al., 2020). Additionally, EEF1D broadly influences various cellular processes including the recognition of damaged proteins, activation of the proteasome degradation system, and regulation of cellular apoptosis (Gao et al., 2020). Importantly, accumulating studies indicate that EEF1D proteins are often overexpressed and are involved in several types of cancer, such as glioma(Xie et al., 2020), ovarian cancer (Xu et al., 2022), oral squamous cell carcinoma (Domingueti et al., 2020; Flores et al., 2016), papillary renal cell carcinoma (Biterge-Sut, 2019), liver cancer (Biterge Sut, 2020), and esophageal cancer (Cheng et al., 2018). It is also involved in inflammatory diseases(Zhao et al., 2023). Thus, aberrant expression of EEF1D

* Corresponding authors.
E-mail addresses: yding202201@163.com (X. Ding), lzhu3596@163.com (L. Zhu).

https://doi.org/10.1016/j.vetmic.2025.110613
Received 23 April 2025; Received in revised form 15 June 2025; Accepted 19 June 2025
Available online 24 June 2025

is pathogenic and potentially associated with a range of diseases.

To our knowledge, the interplay between viral infection and EEF1D signaling remains poorly understood within the virus community. Among the known viruses, influenza A virus (IAV) is the only one for which the involvement of the EEF1D protein in viral replication has been specifically documented. It has been reported that EEF1D interacts with components of the IAV ribonucleoprotein (vRNP) complex and inhibits vRNP assembly, thereby limiting viral replication(Gao et al., 2020). In this study, we investigated the effects of BoAHV1 infection on EEF1D protein expression and explored whether EEF1D plays a role in regulating viral productive infection, as well as the potential underlying mechanisms.

2. Materials and methods

2.1. Virus, cells and plasmid

Human lung carcinoma cell line A549 and bovine kidney MDBK cells were purchased from the Chinese Model Culture Preservation Center in Shanghai, China. Neuro-2A cells were provided as a gift kindly by Dr. Dongli Pan from Zhejiang University. These cells were routinely passaged and maintained in Dulbecco's Modified Eagle Medium (DMEM) supplemented with 10 % fetal bovine serum. BoAHV1 strain NJ-16–1, isolated from commercial bovine semen(Zhu et al., 2017), was propagated in MDBK cells. Aliquots of the virus stocks were stored at −80 °C until required for use. Plasmid pcDNA3.1-EEF1D-Flag that expresses the long isoform of EEF1D was constructed by AZENTA Life Science(Beijing, China). Plasmid pLV4ltr-mCherry-ICP8-Flag that express mCherry-269 fused ICP8 protein was generated by TsingkeBiotechnology (Beijing, China).

2.2. Antibodies

EEF1D rabbit polyclonal antibody (pAb) (cat# A2509), antibody against Flag (cat#AE005), and β-Tubulin rabbit pAb (cat# AC015) were supplied by Abclonal Technology (Woburn, MA, USA). GP73 mouse monoclonal antibody (mAb) (cat# 66331–1-lg) was sourced from Proteintech (Rosemont, IL, USA). LaminA/C mouse mAb (cat# sc-376248) was obtained from Santa Cruz Biotechnology (Dallas, TX, USA). HRP-conjugated goat anti-mouse IgG (cat# BF03001) and HRP-labeled goat anti-rabbit IgG (cat# BF03008) were procured from Biodragon (Suzhou, China). BoAHV1 gD mAb (cat# 1B8-F11), BoAHV1 gC mAb (cat# F2), and goat anti-BoAHV1 serum (cat# PAB-IBR) were supplied by VMRD Inc. (Pullman, WA, USA). Donkey anti-goat IgG H&L (HRP) (cat# ab97110), Alexa Fluor 647-conjugated goat pAb to rabbit IgG (cat# ab150079), and Alexa Fluor 488-conjugated donkey anti-goat IgG (cat# ab150129) were all provided by Abcam (Cambridge, UK).

2.3. siRNAs

Small interfering RNAs (siRNAs) targeting EEF1D, specifically siEEF1D-1: GCAUGAGAAGAUCUGGUUUTT and AAACCAGAUCUUCUCAUGCTT, and siEEF1D-2: GCGUCGACAUUGCUGCUUUTT and AAAGCAGCAAUGUCGACGCTT, along with the scrambled siRNA, were provided by Genepharma (Shanghai, China). Transfection of these siRNAs was carried out using the siRNA-Mate transfection reagent from Genepharma, following the manufacturer's instructions. The efficacy of the siRNAs was assessed by Western blotting.

2.4. Western blot

Cell lysates, encompassing whole cell extracts and specific cellular fractions, such as the cytoplasm, and nucleus, were prepared using RIPA lysis buffer, composed of 1x PBS, 1 % NP-40, 0.5 % sodium deoxycholate, and 0.1 % SDS, and supplemented with a protease inhibitor cocktail. These lysates were boiled in Laemmli sample buffer for 10 min, then separated via SDS-PAGE (using 8 % or 10 % gels), and transferred to polyvinylidene fluoride (PVDF) membranes. Immunoreactive bands were visualized using the Clarity Western ECL Substrate from NCM Biotech (cat# P10300).

Band intensities were quantitatively analyzed using the free software Image J program. Statistical significance was determined using a Student's *t*-test with GraphPad Prism software (version 9.0). *P* values of less than 0.05 (denoted as $*p < 0.05$) were considered to indicate statistical significance for the calculations.

2.5. Immunofluorescence assay (IFA)

MDBK cells, seeded into the 24-well plates containing coverslip, were either mock infected or infected with BoAHV1 at a multiplicity of infection (MOI) of 1 for 24 h. The cells were then fixed with a 4 % solution of paraformaldehyde in PBS for 10 min at room temperature, permeabilized with 0.25 % Triton X-100 in PBS for 5 min at room temperature, and blocked with 1 % BSA in PBST for 1 h. Following this, the cells were incubated with the specified primary antibodies in 1 % BSA in PBST overnight at 4°C. After three washes, the cells were incubated with secondary antibodies conjugated to different fluorescent dyes for 1 h in the dark at room temperature. Another three washes were performed, followed by DAPI (4′,6-diamidino-2-phenylindole) staining to visualize the nuclei. The slides were then mounted with coverslips using an antifade mounting medium (Electron Microscopy Sciences, cat# 50–247–04). Images were obtained using a confocal microscope (Zeiss).

2.6. Determination of the virus titers

MDBK cells were seeded in 96-well microplates and cultured until they reached approximately 50 % confluence. Serial 10-fold dilutions of virus stocks were prepared in DMEM, and 100 μL of each dilution was added to the wells. Following a 72 h incubation period, when the cytopathic effect (CPE) of BoAHV1 infection became apparent, the total number of CPE-positive wells was counted using an inverted microscope. The results were expressed as $TCID_{50}$/mL, calculated using the Reed-Muench-formula (Reed, 1938).

2.7. DNA extraction and analysis of viral genomic levels by real-time quantitative PCR (qPCR) assay

MDBK cells of confluent in 6-well plates were transfected with 150 pmol of either scrambled siRNA or EEF1D-specific siRNA using transfection reagent siRNA-mate (GenePharma, cat# G04001), following the manufacturer's specifications. At 36 h post transfection, the cells were infected with BoAHV1 at an MOI of 1 for 24 h. Then genomic DNA was extracted using DNA extraction kit (Tiangen, DP304), following the manufacturer's protocols. The purified DNA products served as templates for qPCR to measure viral genomic levels using gene-specific primers as previous studies(Liu et al., 2023a; Zhu and Jones, 2017).

The primer sequences used were as follows: viral DNA polymerase (forward reverse primer 5'- GCGAGTACTGCATCCAAGAT-3' and reverse primer 5'- AATCTGCTGCCCGTCAAA-3'); gC (forward reverse primer 5'-ACTATATTTTCCCTTCGCCCG-3' and reverse primer 5'-TGTGACTTGGTGCCCATG-3'), GAPDH (forward primer: 5' CCATGGAGAAGGCTGGGG-3' and reverse primer: 5' AAGTTGTCATGGATGACC-3'). The analysis of glyceraldehyde-3-phosphate dehydrogenase (GAPDH) mRNA served as an internal control. qPCR was performed on the ABI 7500 fast real-time system (Applied Biosystems, CA). Separate amplification of GAPDH was used to normalize gene expression. The data was analyzed using the $2^{-\Delta\Delta CT}$ method.

2.8. RNA isolation and quantification of EEF1D mRNA by qRT-PCR

To analysis the effects of viral infection on EEF1D mRNA expression,

MDBK cells were either mock infected or infected with BoAHV1(MOI =1) for 24 h. Then the cells were harvested and total RNA was extracted using TRIzol LS reagent (Ambion, cat# 10296010) according to the manufacturer's instructions. One microgram of freshly prepared total RNA was utilized as a template for the synthesis of first-strand cDNA with commercial random hexamer primers, employing the Thermo script™ RT-PCR system Kit (Invitrogen, cat# 11146–024) as per the manufacturer's specifications. The resulting cDNA products were then used as templates for qPCR to measure the mRNA levels of EEF1D using the gene-specific primer (Forward: 5'-ACGCAGAGAAGAAGGCCAAG-3', Reverse: 5'-CCTTGTCATCCTCCACCACA-3') as detailed elsewhere (Zhang et al., 2016). Real-time qPCR was conducted using the ABI 7500 fast real-time system (Applied Biosystems, CA). The expression levels of the tested genes were normalized to that of GAPDH. The data was analyzed using the $2^{-\Delta\Delta CT}$ method.

2.9. Isolation of nuclear proteins

MDBK and Neuro-2A cells, grown to confluence in 100 mm dishes, were either mock infected or infected with the virus at an MOI of 1. At 24 hpi, the cells were harvested and processed for the isolation of subcellular fractions, including cytoplasm and nucleus, using a nuclear extraction kit (Beyotime, Shanghai, China, cat# P0028), following the manufacturer's instructions. Briefly, the collected cells were centrifuged at 600 g for 5 min at 4 ℃ to form a pellet. Reagent A was then added to the pellet at a volume ratio of 1:10. After vortexing intensely for 5 s, the mixture was subjected to an ice bath for 10–15 min. Subsequently, reagent B (1/20 vol of reagent A) was added. The mixture was vortexed intensely for 5 s, placed in an ice bath for 1 min, and vortexed again for 5 s. The solution was then centrifuged at 12,000–16,000 g for 5 min at 4 ℃. The supernatant contained the cytoplasmic proteins, while the pellet represented the nuclear fraction. To extract the nuclear proteins, the pellet was re-suspended in 50 μL of nuclear protein extraction reagent, vortexed intensely for 15–30 s and then subjected to an ice-cold bath for 1–2 min. This vortexing and ice-cold bath process was repeated for a total of 30 min. Finally, the mixture was centrifuged at 12,000–16,000 g for 10 min at 4 ℃. The resulting supernatant contained the released nuclear proteins.

2.10. Statistical analysis

All data analyses were conducted using Prism software 8.3 and IBM SPSS Statistics, version 25. The experimental data are presented as mean value ± standard deviation (SD). A one-way analysis of variance (ANOVA) was used to compare multiple groups. *p*-values less than 0.05 were considered statistically significant.

3. Results

3.1. BoAHV1 productive infection increases EEF1D protein expression in cell cultures

To investigate whether EEF1D plays a role in BoAHV1 productive infection in cell cultures, we initially examined the steady-state levels of EEF1D protein following infection of bovine kidney (MDBK) cells. Our data indicated that EEF1D protein levels significantly increased at the later stages of viral infection (Fig. 1A). Quantitative analysis revealed that at 16 and 24 h post-infection (hpi), the EEF1D protein levels increased to approximately 1.5- and 2.3-fold, respectively, relative to those of the mock-infected control (Fig. 1B). A clear examination of

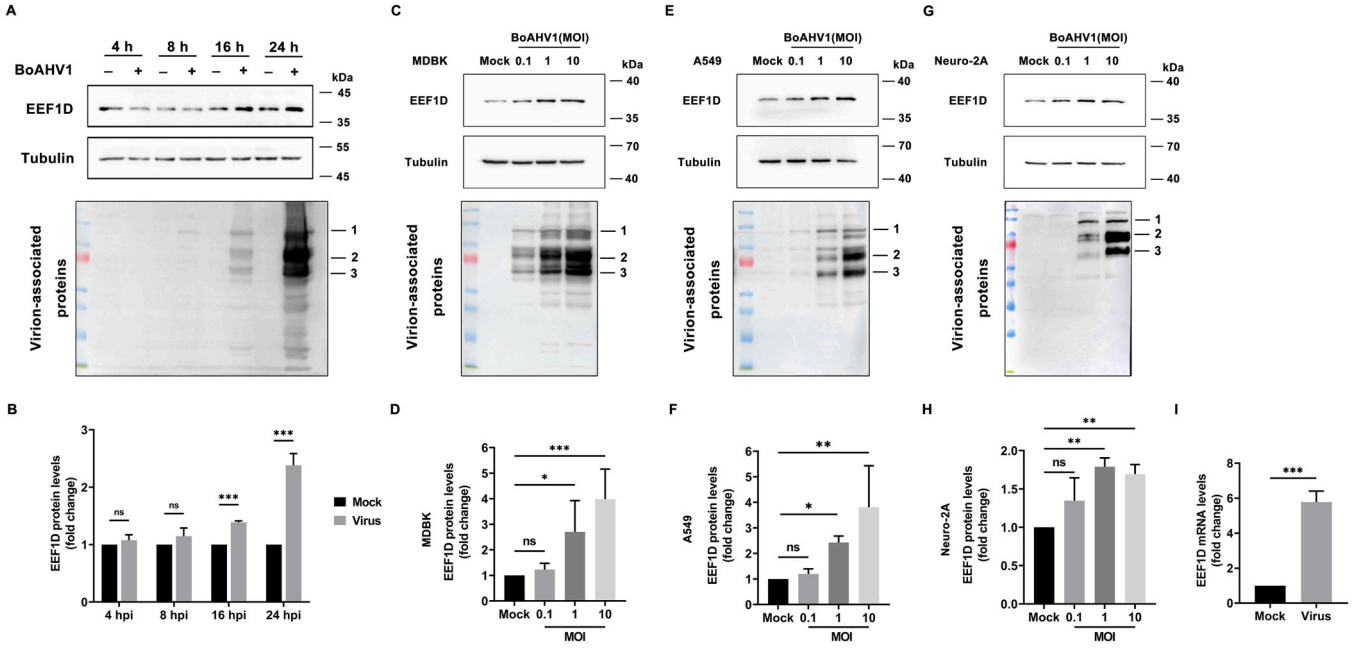

Fig. 1. BoAHV1 infection enhances the expression of EEF1D protein across various cell cultures. (A) MDBK cells were either mock infected or infected with BoAHV1 at an MOI of 1. After infection for 4, 8, 16, and 24 h, cell lysates were prepared and subjected to Western blotting analysis using EEF1D specific antibody (Abclonal, cat# A2509, 1:1000), and goat anti-BoAHV1 serum (VMRD, cat# PAB-IBR, 1:5000), respectively. (B, E, and G) MDBK (C), A549 (E), and Neuro-2A(G) cells were either mock infected or infected with BoAHV1 at an MOI of 0.1, 1, and 10, respectively. At 24 hpi, cell lysates were prepared and subjected to Western blotting analysis using EEF1D specific antibody (Abclonal, cat# A2509, 1:1000), β-Tubulin (Abclonal, cat# AC015, 1:6000), and goat anti-BoAHV1 serum (VMRD, cat# PAB-IBR, 1:5000), respectively. Tubulin was probed and served as a protein loading control and for subsequent quantitative analysis. The data presented are representative of three independent experiments. (B, D, F, and H) Band intensities were quantified using the free software Image J. The band intensity of each virus infection was firstly normalized to that of respective tubulin, they were then normalized to the individual control, which were which was arbitrarily set as 1. (I) MDBK cells in 6-well plates were either mock-infected or infected with BoAHV-1 at an MOI of 1 for 24 h. The mRNA was purified and subjected to detection of EEF1D mRNA levels using qRT-PCR. The data presented are representative of three independent experiments, with error bars indicating standard deviations. Significance was determined using a Student *t*-test (ns, not significant; $^{*}p < 0.05$; $^{**}p < 0.01$; $^{***}p < 0.001$).

virion-associated proteins by Western blot at 16 and 24 hpi validates the correlation between viral infection and the varied EEF1 protein expression (Fig. 1A, bottom panels). When MDBK cells were infected with the virus at increasing MOI ranging from 0.1 to 10 for 24 h, EEF1D protein levels progressively increased in a manner that correlated with the increasing MOIs and expression levels of virion-associated protein (Fig. 1C). EEF1D protein levels increased approximately 2.70- and 3.98-fold following infection with MOIs of 1 and 10, respectively (Fig. 1D). Overall, these findings indicate that BoAHV1 productive infection in MDBK cells specifically upregulates EEF1D protein expression at later stages.

To determine whether BoAHV1 infection alters EEF1D protein expression in a cell-type specific manner, both A549 and Neuro-2A were employed for further studies. These non-bovine original cells also support the virus productive infection, albeit with lower efficiency(Cardoso et al., 2016; Cuddington and Mossman, 2015; Fiorito et al., 2020; Qiu et al., 2021; Thunuguntla et al., 2017). Upon infection of A549 cells with the virus at increasing MOIs for 24 h, EEF1D protein levels increased to approximately 2.43- and 3.81-fold following infection at MOIs of 1 and 10, respectively (Fig. 1E and F). EEF1D protein expression in Neuro-2A cells also increased following virus infection for 24 h at MOIs of 1 and 10, respectively (Fig. 1G). Quantitative analysis indicated that the protein levels increased to approximately 1.79- and 1.70-fold after infection for 24 h with MOIs of 1 and 10, respectively (Fig. 1H). The detected viral protein expression further validated that the altered EEF1D protein levels are associated with viral infection (Fig. 1E and G). These findings suggested that BoAHV1 productive infection at later stages enhances EEF1D protein expression in a cell type-independent manner.

To determine whether virus infection promotes EEF1D protein expression partially through alteration of EEF1D mRNA expression, we assessed the changes of EEF1D mRNA levels in virus-infected MDBK cells using qRT-PCR. We found that EEF1D mRNA levels increased approximately 5.79-fold following 24 h of virus infection compared to the mock-infected control (Fig. 1I). This result supports our findings that

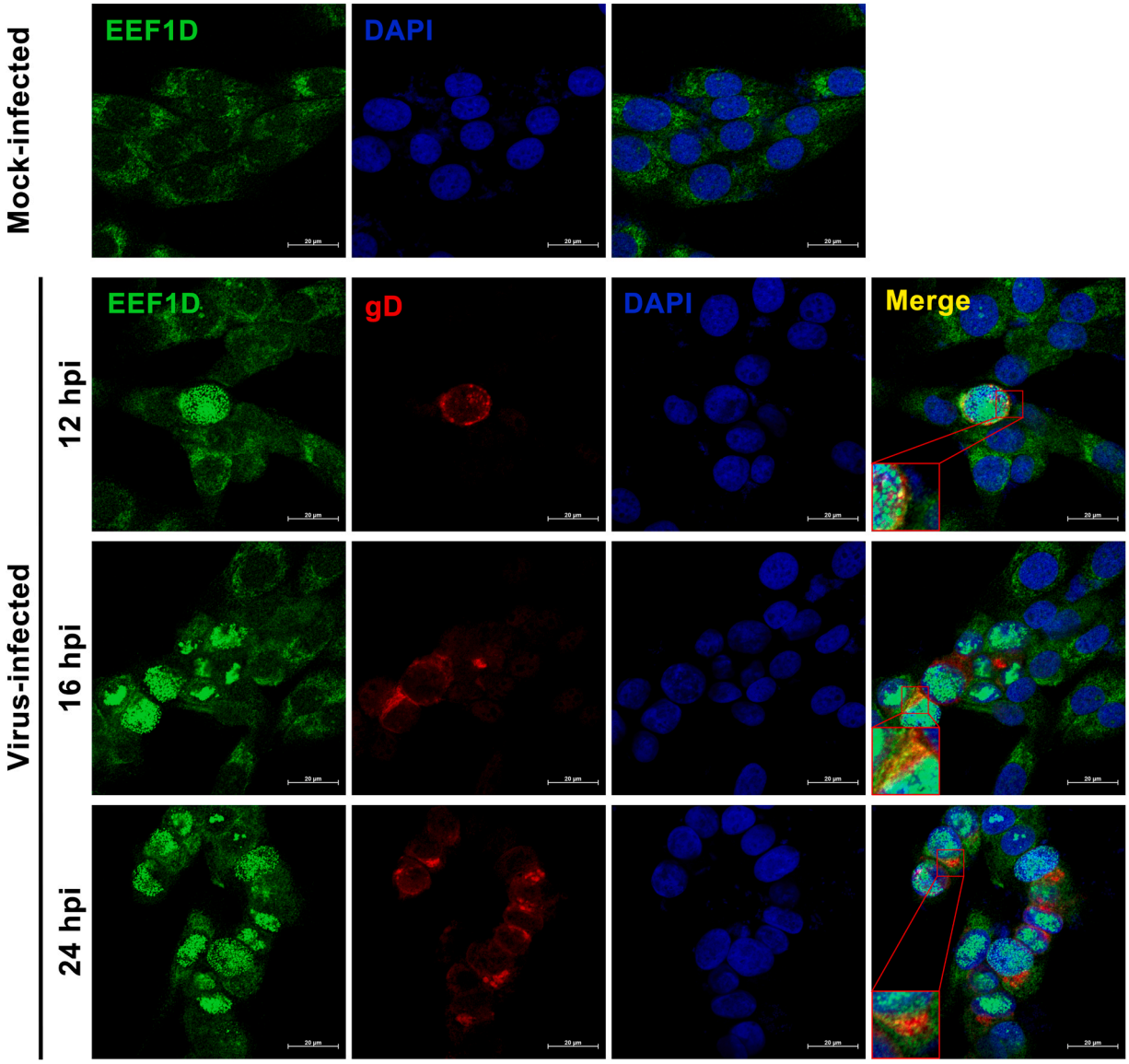

Fig. 2. Examination of EEF1D localization in BoAHV1-infected MDBK cells using IFA assay. MDBK cells were seeded into 24-well plates containing coverslips and cultured until they reached 90 % confluence. The cells were then either mock-infected (upper panels) or infected with BoAHV1 at an MOI of 1 for 12, 16, and 24 h (lower panels). Subsequently, the cells were immunostained with antibodies against the EEF1D protein (green; Abclonal, cat# A2509, 1:100) and the viral protein gD (red; VMRD, cat# 1B8-F11, 1:1000). Nuclei were counterstained with DAPI (4′,6-diamidino-2-phenylindole; blue). Immunofluorescence was visualized and images were captured using confocal microscopy (Zeiss). Zoomed-in images framed in red highlight the typical co-localization of EEF1D with the viral protein gD. These images are representative of results from three independent experiments. Scale bars = 20 μm.

virus infection enhances EEF1D protein expression.

3.2. BoAHV1 productive infection has effects on EEF1D localization in a cell-type specific manner

An immunofluorescence assay (IFA) was conducted to investigate whether BoAHV1 infection in MDBK cell cultures alters the localization of EEF1D proteins. We observed that in mock-infected MDBK cells, EEF1D primarily localized in the cytoplasm (Fig. 2, upper panels). However, in virus-infected cells, the majority of EEF1D protein translocated into the nucleus at 12, 16, and 24 hpi (Fig. 2, lower panels). Notably, at 12 hpi, a subset of EEF1D protein co-localized with viral protein gD puncta in the perinuclear areas, while at 16 and 24 hpi, this co-localization was observed in the cytosol (Fig. 2, zoom-in areas). Overall, viral infection leads to an enhanced accumulation of EEF1D protein in the nucleus, and a subset of viral protein co-localizes with EEF1D in the cytoplasm or perinuclear regions.

IFA was conducted to investigate whether BoAHV1 productive infection in Neruo-2A cell also alters the localization of EEF1D proteins. To this end, the cells were infected for 48 h, then subjected to immunostaining of both virion-associated protein and EEF1D. As a result, we found that in mock-infected Neuro-2A cells, EEF1D mainly located in the nucleus, while the virus productive infection has no dramatic effects on EEF1D localization (Fig. 3). Strikingly, a proportion of EEF1D protein was found to co-localize with virion-associated proteins. While these co-localizations were predominantly observed in the nucleus, a small amount was also detected in the cytoplasm (Fig. 3, lower panels).

In addition, the EEF1D protein was detected in the purified cellular fractions of the nucleus and cytoplasm in both MDBK and Neuro-2A cells. Following viral infection, EEF1D protein levels in the nucleus increased by approximately 2.2-fold in MDBK cells and 3.13-fold in Neuro-2A cells (Fig. 4). Virus productive infection led to a decreased accumulation of EEF1D protein levels in the cytoplasmic fractions of MDBK cells, but no significant change was observed in Neuro-2A cells (Fig. 4). Relative to the mock-infected control, EEF1D protein levels decreased to approximately 51.7 % in virus-infected Neuro-2A cells (Fig. 4 D). Tubulin and Lamin A/C were used as markers for cytoplasmic and nuclear proteins, respectively. The absence of tubulin in the nuclear fractions indicated that the isolated nuclear protein was free from cytosolic protein contamination (Fig. 4 A and B), thereby validating our finding that viral infection enhances the accumulation of EEF1D protein in the nucleus, as demonstrated by immunofluorescence assay (IFA).

Thus, BoAHV1 productive infection in cell cultures differentially affects EEF1D localization in a cell-type-specific manner. Moreover, EEF1D is potentially associated with viral proteins in both MDBK and Neuro-2A cells.

3.3. A proportion of EEF1D is localized in both mitochondria and the Golgi apparatus in virus infected MDBK cells

Literature has demonstrated that in response to infections by α-herpesviruses, such as HSV-1 and BoAHV1, both mitochondria and the Golgi apparatus migrate to the perinuclear region (Liu et al., 2023b; Murata et al., 2000), exhibiting a localization profile similar to that observed for the cytoplasmic EEF1D protein. However, the localization of EEF1D to either mitochondria or the Golgi apparatus has not been reported. Here, mitochondria were stained using Mito-Tracker Deep Red, and Golgi apparatus was immunostained using antibodies against the Golgi-specific marker protein GP73 in both mock-infected and virus-infected MDBK cells. Then EEF1D proteins were probed by IFA in these cells. As a result, a portion of the EEF1D protein was clearly detected within the mitochondria, regardless of viral infection (Fig. 5A). Furthermore, a subset of EEF1D protein was found to co-localize well with GP73, irrespective of viral infection, indicating its accumulation in the Golgi apparatus (Fig. 5B). Therefore, a subset of the EEF1D protein is localized in both the Golgi apparatus and mitochondria, which may explain why the localization profile of EEF1D in virus-infected cytosol resembles that of both the Golgi apparatus and mitochondria.

3.4. EEF1D is potentially involved in the regulation of ICP8 protein

It is well established that viral replication compartments (RCs) are

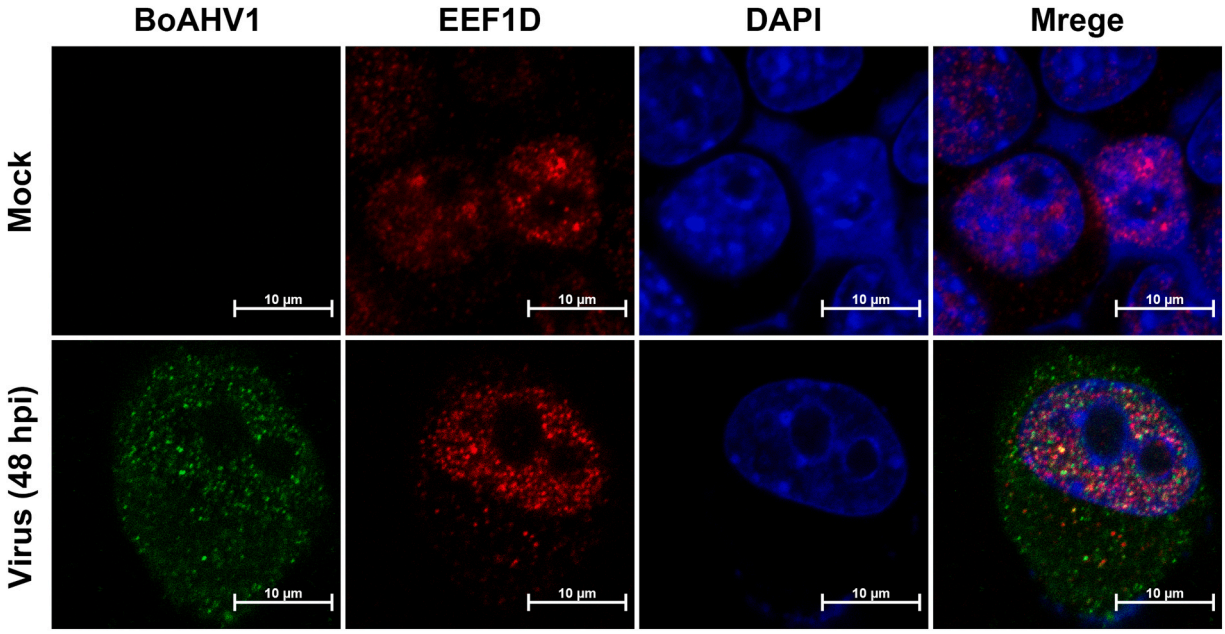

Fig. 3. Examination of EEF1D localization in BoAHV1-infected Neuro-2A cells using IFA assay. Neuro-2A cells were seeded into 24-well plates containing coverslips and cultured until they reached 90 % confluence. The cells were then either mock-infected (upper panels) or infected with BoAHV1 at an MOI of 1 for 48 h (lower panels). Subsequently, the cells were immunostained with an antibody against the EEF1D protein (green; Abclonal, cat# A2509, 1:100) and goat anti-BoAHV1 serum (VMRD, cat# PAB-IBR, 1:1000). Nuclei were counterstained with DAPI (4′,6-diamidino-2-phenylindole; blue). Immunofluorescence was visualized and images were captured using confocal microscopy (Zeiss). These images are representative of results from three independent experiments. Scale bars = 10 μm.

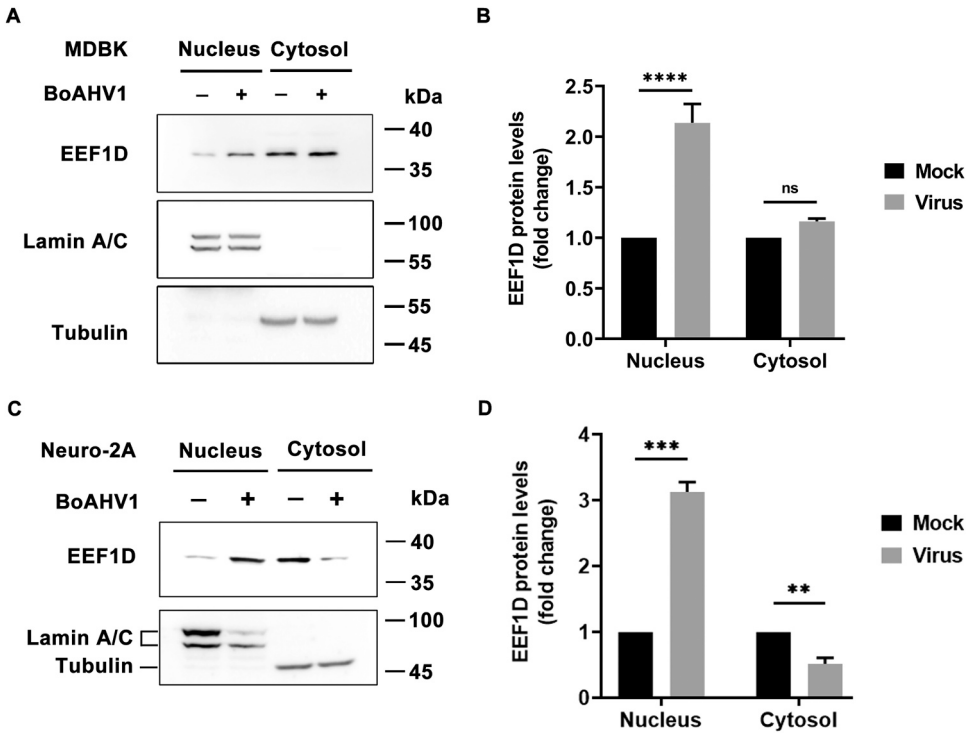

Fig. 4. Examination of the impact of BoAHV1 infection on the nuclear accumulation of EEF1D proteins. MDBK(A) and Neuro-2A(C) cells in 100 mm dishes were either mock-infected or infected with BoAHV1 at an MOI of 1 for 24 and 36 h, respectively. The cells were then collected to isolate the cytoplasm and nuclear fraction using a commercial kit (Beyotime Biotechnology, cat# P0027), following the manufacturer's protocol. The lysates of both nucleus and cytosol were subjected to Western blot assay using antibodies against EEF1D (Abclonal, cat# A2509, 1:1000), Lamin A/C(Santa Cruz Biotechnology, cat# sc-376,248, 1:8000), and β-Tubulin (Abclonal, cat# AC015, 1:6000). β-Tubulin and Lamin A/C served as markers for cytoplasmic and nuclear proteins, respectively, in addition to being protein loading controls. The data presented are representative of three independent experiments. (B and D) The band intensity was analyzed using the free software Image J. The intensity of the band was first normalized to that of the respective Lamin A/C or β-Tubulin, and then normalized to the individual control, which was arbitrarily set to 1. The data presented are representative of three independent experiments, with error bars indicating standard deviations. Significance was determined using a Student's *t*-test (*$p < 0.05$).

formed in the nuclei of herpesvirus-infected cells, serving as sites for viral DNA replication and late gene transcription(Chang et al., 2011; de Bruyn Kops and Knipe, 1988). The viral protein ICP8, which localizes to RCs, is commonly used as a marker for these RCs(de Bruyn Kops and Knipe, 1988). In our IFA assays, we observed that EEF1D immunostaining forms numerous foci within the nuclei of virus-infected cells (Fig. 2, zoom-in areas). This led us to investigate whether nuclear EEF1D is associated with RCs.

Of note, there are four EEF1D isoforms, including three short isoforms and one long isoform, based on their polypeptide length. The short isoforms are primarily located in the cytoplasm and act as translation elongation factors. The single long isoform is typically found in both the cytoplasm and nucleus and functions as a transcription factor, reviewed by Xu et al. (2021). To address this question, plasmids encoding mCherry-fused ICP8 and the long isoform of Flag-tagged EEF1D were transfected into Neuro-2A cells, either individually or in combination. Neuro-2A cells were chosen for this experiment due to their higher transfection efficiency compared to MDBK cells. Additionally, Neuro-2A cells support productive viral infection, making them an ideal model for this study(Cardoso et al., 2016; Cuddington and Mossman, 2015; Fiorito et al., 2020; Qiu et al., 2021; Thunuguntla et al., 2017). When plasmid pLV4ltr-mCherry-ICP8-Flag was transfected into Neuro-2A cells alone, the protein primarily localized to the nucleus (Fig. 6A). However, upon co-transfection of ICP8 and Flag-tagged EEF1D, ICP8 was detected in both the cytosol and nucleus in some cells, or exclusively in the nucleus. Additionally, ICP8 foci were observed in a subset of cells (Fig. 6B). Meanwhile, the EEF1D protein was detected in both the nucleus and cytosol (Fig. 6B, upper panels), predominantly in the cytosol (Fig. 6B, middle panels), or exclusively in the nucleus (Fig. 6B, bottom panels). Notably, co-localization of ICP8 and EEF1D was observed in the cytosol (Fig. 6B, upper and middle panels). Interestingly, when the plasmid pLV4ltr-mCherry-ICP8-Flag was transfected into MDBK cells and subsequently infected with the virus for 24 h, a portion of the ICP8 protein was found to localize in the nucleus, where it frequently co-localized with EEF1D (Fig. 7). These findings suggested that EEF1D is capable of association with viral protein ICP8. Specifically, the association was observed in the cytosol in uninfected cells, while it was detected in the nucleus in the context of viral infection. Thus, a portion of the EEF1D protein may be recruited into viral RCs through its interaction with ICP8.

3.5. *EEF1D plays an important role in BoAHV1 productive infection in cell cultures*

To elucidate the roles of EEF1D in BoAHV1 productive infection, two commercially available small interfering RNAs (siRNAs), designated as siEEF1D-1 and siEEF1D-2, were employed in this study. As demonstrated in Fig. 8A, transfection with either siEEF1D-1 or siEEF1D-2 resulted in a significant decrease in EEF1D protein expression in MDBK cells. Knockdown of EEF1D protein expression significantly reduced viral replication at all detected time points, including 24, 36, and 48 hpi. Specifically, the virus titers were reduced by 0.8- to 1-log by each of the two siRNA, respectively (Fig. 8B). Additionally, siRNA-mediated knockdown of EEF1D expression reduced viral genome levels, as determined by quantitative PCR (qPCR). Specifically, the viral genome levels were reduced to approximately 66.9 % and 75.5 % when assessed using primers specific for viral DNA polymerase and gC, respectively (Fig. 8C). When glycoproteins gC and gD were analyzed via

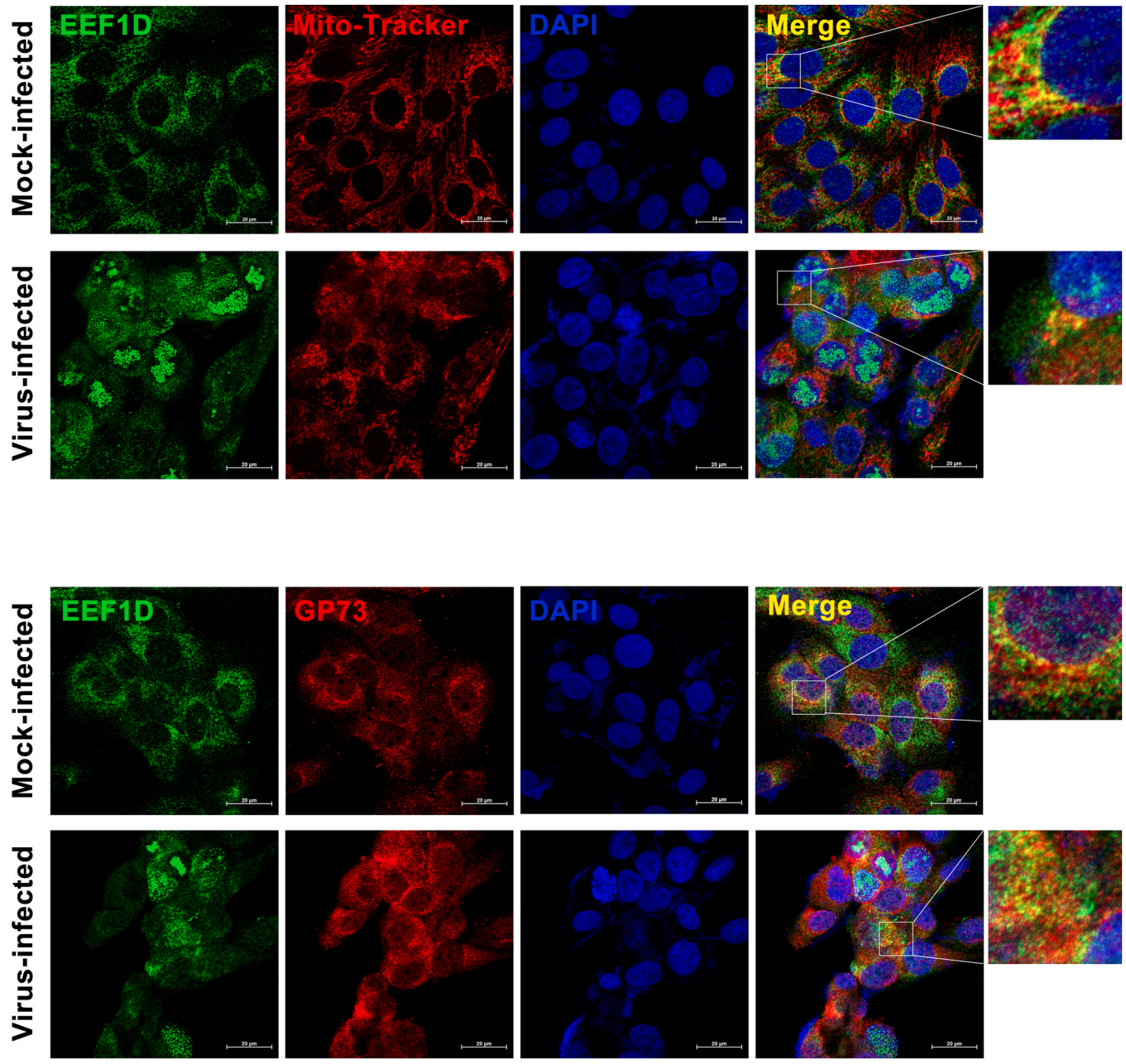

Fig. 5. Identification of EEF1D protein in mitochondria and Golgi apparatus. (A) MDBK cells in 24-well plates containing coverslips were either mock-infected or infected with BoAHV1 at an MOI of 1 for 24 h. Subsequently, EEF1D protein was immunostained with antibodies against EEF1D (Green, Abclonal, cat# A2509, 1:100). The mitochondria were probed using Mito-Tracker Deep Red FM (Beyotime, cat# C1032). Nuclei were stained with DAPI (blue). (B) MDBK cells in 24-well plates containing coverslips were either mock-infected or infected with BoAHV1 at an MOI of 1 for 24 h. Subsequently, the cells were immunostained with antibodies against EEF1D (Green, Abclonal, cat# A2509, 1:100) and GP73 (Red, Proteintech, cat# 66331, 1:200). GP73 was used as an indicator of the Golgi apparatus. Nuclei were stained with DAPI (blue). The immunofluorescence was visualized, and images were captured using confocal microscopy (Zeiss). These images are representative of three independent experiments. Scale bars = 20 μm.

Western blot using commercial available monoclonal antibodies, both were fund to be significantly reduced as a result of siRNA-mediated knockdown of EEF1D expression (Fig. 8D). Quantitative analysis revealed that gC protein levels were reduced to approximately 71.14 % and 49.60 %, while gD protein levels dropped to about 63.43 % and 62.12 % by siEEF1D-1 and siEEF1D-2, respectively (Fig. 8E). Of note, two bands of the gD protein were also detected by this gD-specific monoclonal antibody (VMRD, cat# 1B8-F11), as previously shown elsewhere (Zhao et al., 2025), presumably representing different glycosylation states. Collectively, these data suggest that EEF1D signaling play an important role in BoAHV1 productive infection.

4. Discussion

It has been reported that there are four EEF1D isoforms, including three short isoforms primarily located in the cytoplasm and one long isoform found in both the cytosol and nucleus, reviewed by Xu et al. (2021). The long isoform is particularly enriched in neurons (Kaitsuka et al., 2018; Xu et al., 2021). In this study, the antibody used recognized all four isoforms. However, our Western blot data indicated that the detected EEF1D in both MDBK and Neuro-2A cells corresponds to one of the short isoforms, as inferred from the molecular weights. Our studies revealed that BoAHV1 productive infection in MDBK cell cultures

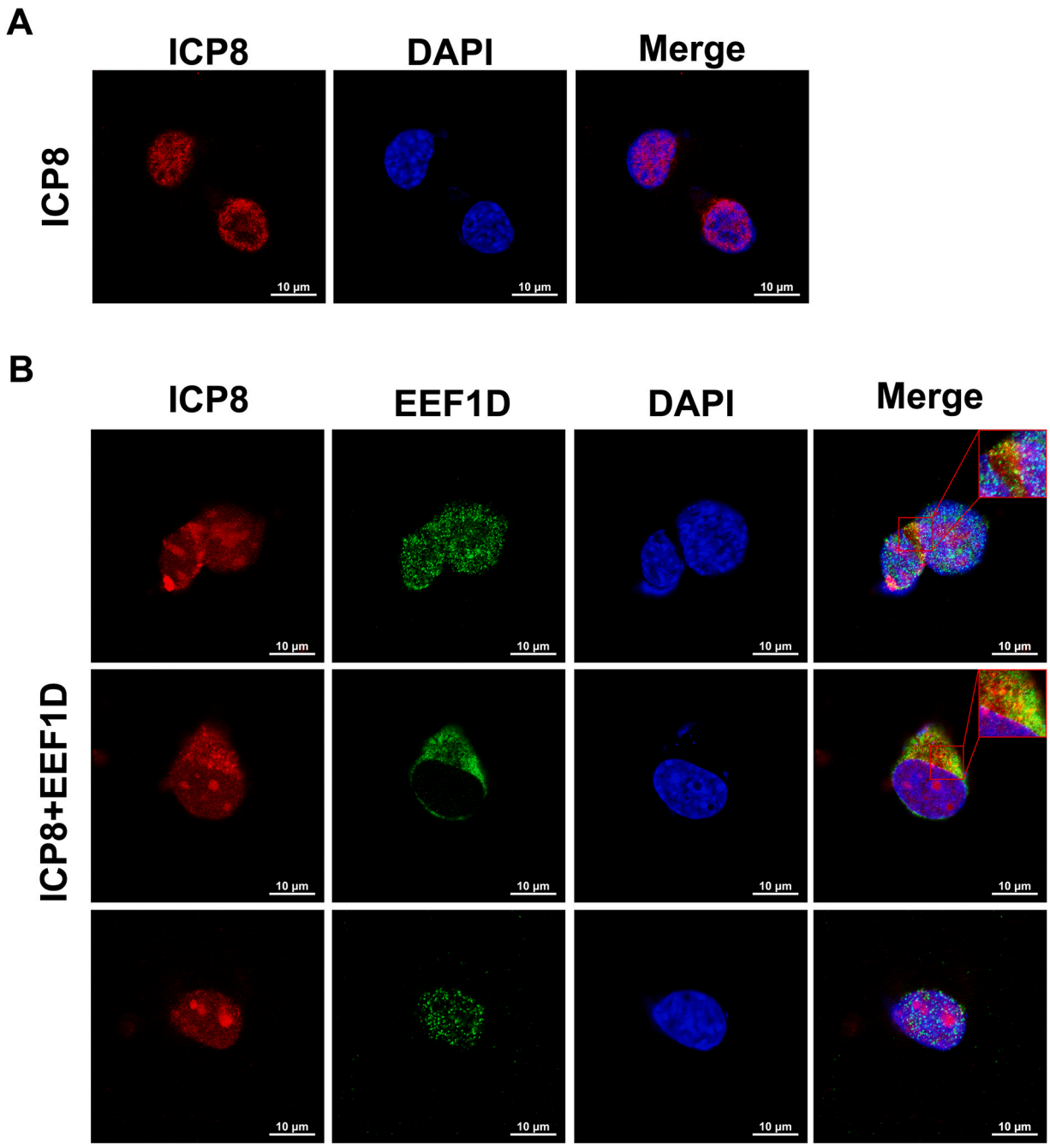

Fig. 6. Examination of the interaction between EEF1D and viral protein ICP8 using plasmid transfection. (A) Neuro-2A cells in 24-well plates containing coverslips were transfected with 1 μg of the plasmid pLV4ltr-mCherry-ICP8-Flag (Tsingke) using Lipofectamine 3000. At 48 h post-transfection, the expression of ICP8 were immunostained with an anti-Flag antibody (Red; Abclonal, cat# AE005, 1:1000). Nuclei were stained with DAPI. (B) Neuro-2A cells were co-transfected with 1 μg of plasmids expressing FLAG-tagged EEF1D and mCherry-Flag-tagged ICP8 using Lipofectamine 3000. At 48 h post-transfection, cells were immunostained with an anti-EEF1D antibody (Green; Abclonal, cat# A2509, 1:100). Nuclei were stained with DAPI. EEF1D (Green) and mCherry-Flag-tagged ICP8 (Red) were then visualized under confocal microscopy (Zeiss). These images are representative of three independent experiments. Scale bars = 10 μm.

increases EEF1D protein expression and promotes its translocation into the nucleus (Figs. 1 and 2). Thus, the short isoform of EEF1D in MDBK cells, recognized by this antibody, is also capable of translocating into the nucleus under specific conditions, such as during BoAHV1 productive infection. In addition, EEF1D protein expressed in Neuro-2A cells is primarily localized in the nucleus, regardless of virus infection (Fig. 4). This observation further confirms that the short isoform of EEF1D is capable of nuclear translocation.

Within the virology community, the role of EEF1D in viral replication and pathogenicity has only been documented in the case of the influenza A virus (IAV). It has been reported that EEF1D limits IAV replication (Gao et al., 2020). Here, we demonstrated that siRNA-mediated knockdown of EEF1D results in reduced viral titers, diminished viral genome levels, and decreased expression of viral proteins, including gC and gD(Fig. 8). Clearly, the influence of EEF1D signaling on BoAHV1 replication differs from its effects on IAV replication (enhancement vs. suppression). Notably, IAV is an RNA virus, whereas BoAHV1 is a DNA virus. Thus, EEF1D signaling may impact virus replication in a virus-genome-type-specific or virus-specific manner.

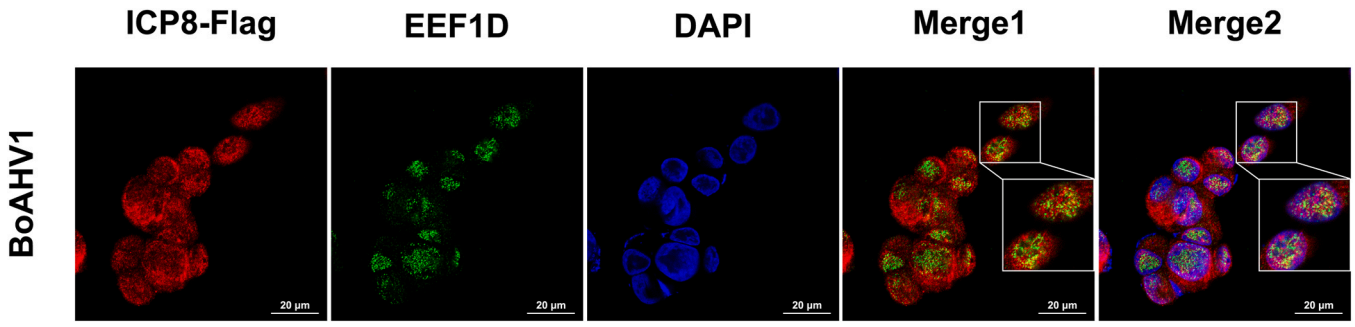

Fig. 7. Examination of the interaction between EEF1D and viral protein ICP8 in virus infected cells using plasmid transfection. MDBK cells in 24-well plates containing coverslips were transfected with 1 μg of plasmid pLV4ltr-mCherry-ICP8-Flag using Lipofectamine 3000. At 36 h post-transfection, cells were infected with BoAHV1 at an MOI of 1. After infection for 24 h, cells were immunostained with an anti-EEF1D antibody (Green; Abclonal, cat# A2509, 1:100), and Flag antibody (Red; Abclonal, cat#AE005, 1:1000). Nuclei were stained with DAPI. EEF1D (Green) and ICP8 (Red) were then visualized under confocal microscopy (Zeiss). These images are representative of three independent experiments. Scale bars = 20 μm.

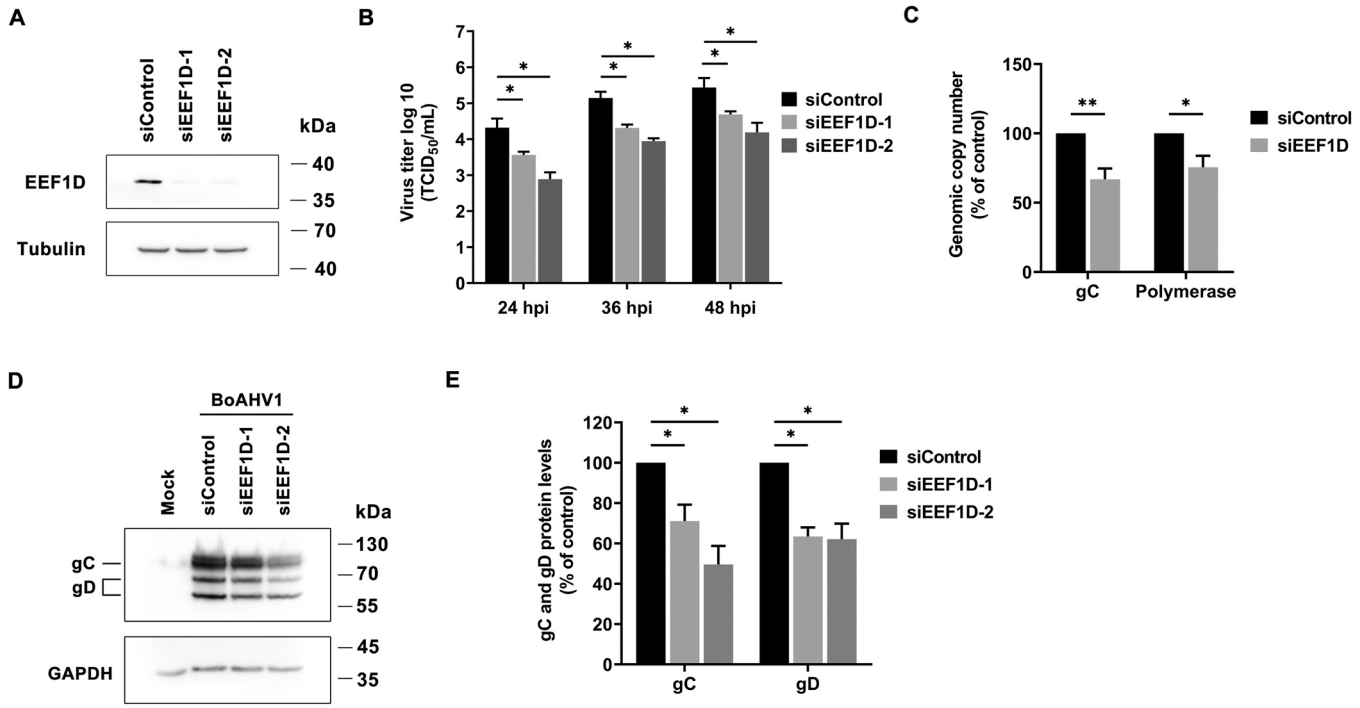

Fig. 8. EEF1D plays an important role in BoAHV1 productive infection. (A) MDBK cells in 6-well plates were transfected with either scrambled siRNA (150 pmol) or two individual siRNAs targeting EEF1D (150 pmol), referred to as siEEF1D-1, siEEF1D-2, respectively. At 48 h post transfection, cell lysates were prepared and subjected to Western blot to detect EEF1D protein levels via Western blot using an antibody against EEF1D (Abclonal, cat# A2509, 1:100). (B-D) MDBK cells in 6-well plates were transfected with either scrambled siRNA (150 pmol) or siEEF1D (150 pmol). At 36 h, cells were infected with BoAHV1 at an MOI of 1. After infection for 24, 36 and 48 h, viral yields in the supernatants were measured with results expressed as $TCID_{50}$/mL(B). Simultaneously, at 24 hip, the cells were collected to extract total RNA for the detection of viral mRNA using qRT-PCR (C), or to prepare cell lysates for Western blot analysis using antibodies against gC (VMRD, cat# F2, 1:2000) and gD (VMRD, cat# 1B8-F11, 1:3000). (D), respectively. (E and F) The band intensities of both gC (E) and gD (F) were quantified using the free software ImageJ. The intensity of each band was first normalized to that of the respective loading control GAPDH, and then normalized to that of the control transfected with scramble siRNA, which was arbitrarily set to 100 %. The data shown are representative of three independent experiments, with error bars representing standard deviations. Significance was assessed using a Student's *t*-test (* $p < 0.05$, ** $p < 0.01$).

Our IFA analysis demonstrated that a portion of EEF1D co-localizes with the viral protein, such as gD, in the cytosol of virus-infected MDBK cells, and primarily in the nucleus of virus-infected Neuro-2A cells (Figs. 3 and 4). In addition, EEF1D co-localizes with a subset of ICP8 puncta in the cytosol, and inhibits the translocation of the viral protein ICP8 to nucleus, as characterized by co-transfection of the EEF1D and ICP8 plasmids (Fig. 6). However, in the context of virus infection, the puncta of ICP8 co-localize well with that of EEF1D in the nucleus (Fig. 7). Given that ICP8 puncta serve as markers of viral replication compartments (RCs), which are essential for viral replication (de Bruyn Kops and Knipe, 1988), it is possible that EEF1D recruited into these RCs may play significant role in the virus replication process. This hypothesis warrants further investigation in future studies, particularly once suitable ICP8 antibodies and specific EEF1D inhibitors become available.

Accumulating studies suggests that EEF1D signaling is involved in the pathogenicity of various diseases, especially in the progression of numerous malignant tumors, by modulating cell proliferation, tumor growth, and tumor invasion (Cheng et al., 2018). And it is well established that viral RCs, formed in the nuclei of infected cells, serve as critical sites for herpesvirus DNA replication and late gene transcription. The viral protein ICP8 is a key component of RCs and plays a crucial role

in the virus replication cycle(Chang et al., 2011; de Bruyn Kops and Knipe, 1988). Given that ICP8-related RCs are essential for the replication of all herpesviruses, we hypothesize that EEF1D may play a significant role across all herpesviruses. Therefore, EEF1D may broadly affect the infection of other herpesviruses, making it a potential target for the development of novel anti-herpesvirus drugs. This possibility warrants further exploration in future studies. Notably, it has been reported that the EEF1D protein interacts with viral ribonucleoprotein (vRNP) subunits, a mechanism that limits influenza A virus (IAV) replication (Gao et al., 2020). Here, we found that EEF1D is potentially associated with a range of viral proteins, such as viral proteins gD and ICP8 (Figs. 3, 6, and 7). Here, we found that EEF1D is potentially associated with a range of viral proteins, such as gD and ICP8 (Figs. 3, 6, and 7). Of note, our Western blot data showed that the EEF1D detected in MDBK cells by the antibody corresponds to the short isoforms (Fig. 1), while the plasmid-expressed EEF1D corresponds to the long isoform, they both are capable of associating with viral proteins (gD vs. ICP8). Thus, the association of EEF1D with viral proteins may represent a potential conserved mechanism for regulating viral replication processes.

We have previously reported that BoAHV1 productive infection in cell cultures leads to a decrease in mitochondrial biogenesis. This reduction may result in the overproduction of inflammatory mediators and reactive oxygen species (ROS), which could potentially contribute to viral pathogenicity (Lin et al., 2025; Zhu et al., 2016). Additionally, we have shown that the Golgi apparatus serves as a crucial site for the transport of BoAHV1 virions to the cell membrane (Liu et al., 2023b). In this study, for the first time, we report that a subset of EEF1D proteins localizes to mitochondria and the Golgi apparatus in MDBK cells, regardless of viral infection (Fig. 5). Future studies would focus on elucidating whether and how EEF1D is involved in mitochondrial biogenesis and virion transport from the Golgi to the cell membrane in virus-infected cells. This line of investigation may provide valuable insights into the mechanisms underlying BoAHV1 pathogenesis and host-virus interactions.

In summary, this study provides the first evidence that EEF1D plays a crucial role in BoAHV1 productive infection. Importantly, we report that EEF1D is potentially associated with viral proteins, such as gD and ICP8. Notably, a portion of EEF1D is recruited into replication compartments (RCs), which is essential for viral replication. Thus, EEF1D may serve as a potential target for the development of anti-herpesvirus drugs. Furthermore, we discovered that a subset of EEF1D protein localizes to the Golgi apparatus and mitochondria, both of which are critical for the viral replication cycle and pathogenicity. These findings will expand our understanding of the mechanisms underlying virus productive infection involving the EEF1D protein.

CRediT authorship contribution statement

Yuanshan Luo: Methodology, Investigation, Formal analysis. **Xiaotian Fu:** Methodology, Investigation, Formal analysis, Data curation. **Liqian Zhu:** Writing – review & editing, Writing – original draft, Visualization, Validation, Supervision, Resources, Project administration, Funding acquisition, Data curation, Conceptualization. **Xiuyan Ding:** Writing – review & editing, Writing – original draft, Supervision, Software, Resources, Conceptualization. **Bin Hou:** Visualization, Validation, Methodology, Investigation, Formal analysis, Data curation.

Declaration of Competing Interest

The authors declare no conflicts of interest

Acknowledgments

This research was supported by the National Natural Science Foundation of China (Grant No. 32373006 to L.Q. Z), Foundation of Science and Technology of Hebei Province (Grant No. 246Z2401G), Key Research Program for Agriculture Development of Shijiazhuang City (Grant No.241500152 A), and the Cow innovation group of Hebei Agriculture Research System (Grant No. HBCT2024230201 to L.Q.Z).

References

Andersen, G.R., Pedersen, L., Valente, L., Chatterjee, I., Kinzy, T.G., Kjeldgaard, M., Nyborg, J., 2000. Structural basis for nucleotide exchange and competition with tRNA in the yeast elongation factor complex eEF1A:eEF1Balpha. Mol. Cell 6, 1261–1266.

Biterge Sut, B., 2020. Data article on genes that share similar expression patterns with EEF1 complex proteins in hepatocellular carcinoma. Data Brief. 29, 105162.

Biterge-Sut, B., 2019. Alterations in Eukaryotic Elongation Factor complex proteins (EEF1s) in cancer and their implications in epigenetic regulation. Life Sci. 238, 116977.

de Bruyn Kops, A., Knipe, D.M., 1988. Formation of DNA replication structures in herpes virus-infected cells requires a viral DNA binding protein. Cell 55, 857–868.

Cardoso, T.C., Rosa, A.C., Ferreira, H.L., Okamura, L.H., Oliveira, B.R., Vieira, F.V., Silva-Frade, C., Gameiro, R., Flores, E.F., 2016. Bovine herpesviruses induce different cell death forms in neuronal and glial-derived tumor cell cultures. J. Neurovirol. 22, 725–735.

Chang, L., Godinez, W.J., Kim, I.H., Tektonidis, M., de Lanerolle, P., Eils, R., Rohr, K., Knipe, D.M., 2011. Herpesviral replication compartments move and coalesce at nuclear speckles to enhance export of viral late mRNA. Proc. Natl. Acad. Sci. USA 108, E136–144.

Chase, C.C.L., Fulton, R.W., O'Toole, D., Gillette, B., Daly, R.F., Perry, G., Clement, T., 2017. Bovine herpesvirus 1 modified live virus vaccines for cattle reproduction: balancing protection with undesired effects. Vet. Microbiol. 206, 69–77.

Cheng, D.D., Li, S.J., Zhu, B., Zhou, S.M., Yang, Q.C., 2018. EEF1D overexpression promotes osteosarcoma cell proliferation by facilitating Akt-mTOR and Akt-bad signaling. J. Exp. Clin. Cancer Res. 37, 50.

Cuddington, B.P., Mossman, K.L., 2015. Oncolytic bovine herpesvirus type 1 as a broad spectrum cancer therapeutic. Curr. Opin. Virol. 13, 11–16.

Dever, T.E., Green, R., 2012. The elongation, termination, and recycling phases of translation in eukaryotes. Cold Spring Harb. Perspect. Biol. 4, a013706.

Domingueti, C.B., Castilho, D.A.Q., de Oliveira, C.E., Janini, J.B.M., Gonzalez-Arriagada, W.A., Salo, T., Coletta, R.D., Paranaiba, L.M.R., 2020. Eukaryotic translation elongation factor 1delta, N-terminal propeptide of type I collagen and cancer-associated fibroblasts are prognostic markers of oral squamous cell carcinoma patients. Oral. Surg. Oral. Med Oral. Pathol. Oral. Radiol. 130, 700–707 e702.

Fiorito, F., Nocera, F.P., Cantiello, A., Iovane, V., Lambiase, S., Piccolo, M., Ferraro, M. G., Santamaria, R., De Martino, L., 2020. Bovine herpesvirus-1 infection in mouse neuroblastoma (Neuro-2A) cells. Vet. Microbiol. 247, 108762.

Flores, I.L., Kawahara, R., Miguel, M.C., Granato, D.C., Domingues, R.R., Macedo, C.C., Carnielli, C.M., Yokoo, S., Rodrigues, P.C., Monteiro, B.V., Oliveira, C.E., Salmon, C. R., Nociti Jr., F.H., Lopes, M.A., Santos-Silva, A., Winck, F.V., Coletta, R.D., Paes Leme, A.F., 2016. EEF1D modulates proliferation and epithelial-mesenchymal transition in oral squamous cell carcinoma. Clin. Sci. 130, 785–799.

Fulton, R.W., d'Offay, J.M., Landis, C., Miles, D.G., Smith, R.A., Saliki, J.T., Ridpath, J.F., Confer, A.W., Neill, J.D., Eberle, R., Clement, T.J., Chase, C.C., Burge, L.J., Payton, M.E., 2016. Detection and characterization of viruses as field and vaccine strains in feedlot cattle with bovine respiratory disease. Vaccine 34, 3478–3492.

Gao, Q., Yang, C., Ren, C., Zhang, S., Gao, X., Jin, M., Chen, H., Ma, W., Zhou, H., 2020. Eukaryotic translation elongation factor 1 delta inhibits the nuclear import of the nucleoprotein and PA-PB1 heterodimer of influenza A virus. J. Virol. 95.

Hodgson, P.D., Aich, P., Manuja, A., Hokamp, K., Roche, F.M., Brinkman, F.S., Potter, A., Babiuk, L.A., Griebel, P.J., 2005. Effect of stress on viral-bacterial synergy in bovine respiratory disease: novel mechanisms to regulate inflammation. Comp. Funct. Genom. 6, 244–250.

Iscaro, C., Cambiotti, V., Petrini, S., Feliziani, F., 2021. Control programs for infectious bovine rhinotracheitis (IBR) in European countries: an overview. Anim. Health Res. Rev. 22, 136–146.

Jones, C., 2019. Bovine herpesvirus 1 counteracts immune responses and immune-surveillance to enhance pathogenesis and virus transmission. Front. Immunol. 10, 1008.

Jones, C., Chowdhury, S., 2007. A review of the biology of bovine herpesvirus type 1 (BHV-1), its role as a cofactor in the bovine respiratory disease complex and development of improved vaccines. Anim. Health Res. Rev. 8, 187–205.

Kaitsuka, T., Kiyonari, H., Shiraishi, A., Tomizawa, K., Matsushita, M., 2018. Deletion of long isoform of eukaryotic elongation factor 1Bdelta leads to audiogenic seizures and aversive stimulus-induced long-lasting activity suppression in mice. Front. Mol. Neurosci. 11, 358.

Lin, J., Fu, X., Li, X., Ding, X., Li, S., Fiorito, F., Zhu, L., 2025. The depletion of TFAM and p-beta-catenin(S552) in mitochondria in response to BoAHV-1 productive infection leads to decreased mitochondrial biogenesis. Vet. Microbiol. 304, 110454.

Liu, C., Lin, J.Y., Yang, H., Li, N.X., Tang, L.K., Neumann, D., Ding, X.Y., Zhu, L.Q., 2023a. NFAT5 restricts bovine herpesvirus 1 productive infection in MDBK cell cultures. Microbiol Spectr. 11.

Liu, C., Yuan, W., Yang, H., Ni, J., Tang, L., Zhao, H., Neumann, D., Ding, X., Zhu, L., 2023b. Associating bovine herpesvirus 1 envelope glycoprotein gD with activated phospho-PLC-gamma1(S1248). Microbiol. Spectr. 11, e0196323.

Murata, T., Goshima, F., Daikoku, T., Inagaki-Ohara, K., Takakuwa, H., Kato, K., Nishiyama, Y., 2000. Mitochondrial distribution and function in herpes simplex virus-infected cells. J. Gen. Virol. 81, 401–406.

Muylkens, B., Thiry, J., Kirten, P., Schynts, F., Thiry, E., 2007. Bovine herpesvirus 1 infection and infectious bovine rhinotracheitis. Vet. Res. 38, 181–209.
Petrini, S., Iscaro, C., Righi, C., 2019. Antibody responses to bovine alphaherpesvirus 1 (BoHV-1) in passively immunized calves. Viruses 11.
Qiu, W., Ding, X., Li, S., He, Y., Zhu, L., 2021. Oncolytic bovine herpesvirus 1 inhibits human lung adenocarcinoma A549 cell proliferation and tumor growth by inducing DNA damage. Int J. Mol. Sci. 22.
Reed, L.J., 1938. A simple method of estimating 50 percent endpoints. Am. J. Hyg. 27.
Siddell, S.G., Smith, D.B., Adriaenssens, E., Alfenas-Zerbini, P., Dutilh, B.E., Garcia, M.L., Junglen, S., Krupovic, M., Kuhn, J.H., Lambert, A.J., Lefkowitz, E.J., Lobocka, M., Mushegian, A.R., Oksanen, H.M., Robertson, D.L., Rubino, L., Sabanadzovic, S., Simmonds, P., Suzuki, N., Van Doorslaer, K., Vandamme, A.M., Varsani, A., Zerbini, F.M., 2023. Virus taxonomy and the role of the international committee on taxonomy of viruses (ICTV). J. Gen. Virol. 104.
Thunuguntla, P., El-Mayet, F.S., Jones, C., 2017. Bovine herpesvirus 1 can efficiently infect the human (SH-SY5Y) but not the mouse neuroblastoma cell line (Neuro-2A). Virus Res. 232, 1–5.
Tikoo, S.K., Campos, M., Babiuk, L.A., 1995. Bovine herpesvirus 1 (BHV-1): biology, pathogenesis, and control. Adv. Virus Res. 45, 191–223.
Xie, C., Zhou, M., Lin, J., Wu, Z., Ding, S., Luo, J., Zhan, Z., Cai, Y., Xue, S., Song, Y., 2020. EEF1D promotes glioma proliferation, migration, and invasion through EMT and PI3K/Akt pathway. Biomed. Res. Int. 2020, 7804706.
Xu, Q., Liu, Y., Wang, S., Wang, J., Liu, L., Xu, Y., Qin, Y., 2022. Interfering with the expression of EEF1D gene enhances the sensitivity of ovarian cancer cells to cisplatin. BMC Cancer 22, 628.
Xu, H., Yu, S., Peng, K., Gao, L., Chen, S., Shen, Z., Han, Z., Chen, M., Lin, J., Chen, S., Kang, M., 2021. The role of EEF1D in disease pathogenesis: a narrative review. Ann. Transl. Med. 9, 1600.
Zhang, S., Wu, X., Pan, C., Lei, C., Dang, R., Chen, H., Lan, X., 2016. Identification of novel isoforms of dairy goat EEF1D and their mRNA expression characterization. Gene 581, 14–20.
Zhao, H., Fu, X., Gu, W., Ding, X., Zhua, L., 2025. 53BP1, a known chromatin-associated factor that promotes DNA damage repair, is differentially modulated during bovine herpesvirus 1 infection in vitro and in vivo. Vet. Microbiol. 300, 110334.
Zhao, J., Zhang, Q., Yao, D., Wang, T., Ni, M., Xu, Y., Tang, Z., Liu, Z., 2023. Prenatal LPS exposure promotes allergic airway inflammation via long coding RNA NONMMUT033452.2, and protein binding partner, Eef1D. Am. J. Respir. Cell Mol. Biol. 68, 610–624.
Zhu, L.Q., Jones, C., 2017. The high mobility group AT-hook 1 protein stimulates bovine herpesvirus 1 productive infection. Virus Res. 238, 236–242.
Zhu, L., Yu, Y., Jiang, X., Yuan, W., Zhu, G., 2017. First report of bovine herpesvirus 1 isolation from bull semen samples in China. Acta Virol. 61, 483–486.
Zhu, L., Yuan, C., Zhang, D., Ma, Y., Ding, X., Zhu, G., 2016. BHV-1 induced oxidative stress contributes to mitochondrial dysfunction in MDBK cells. Vet. Res. 47, 47.